ELSEVIER

Journal of Organometallic Chemistry 539 (1997) 9–17

Journal of Organometallic Chemistry

Metal polypyrazolylborates XIII. Solution and solid state NMR study of cyano–mercury(II) polypyrazolylborates. X-ray crystal structure of [HB(3,5-Me_2pz)$_3$]HgCN

Giancarlo Gioia Lobbia [a,*], Patrizio Cecchi [b], Roberto Gobetto [c], Giuseppe Digilio [c], Riccardo Spagna [d], Mercedes Camalli [d]

[a] *Dipartimento di Scienze Chimiche, Università di Camerino, Via S. Agostino 1, I-62032 Camerino, Italy*
[b] *Dipartimento di Agrobiologia ed Agrochimica, Università della Tuscia, Via S.C. De Lellis, I-01100 Viterbo, Italy*
[c] *Dipartimento di Chimica Inorganica, Chimica Fisica e Chimica dei Materiali, Università di Torino, Via P. Giuria 7, I-10125 Torino, Italy*
[d] *Istituto di Strutturistica Chimica "G. Giacomello" CNR, CP10 I-00016 Monterotondo Stazione (Roma), Italy*

Received 21 May 1996; accepted 30 September 1996

Abstract

Complexes of the cyanomercury cation with various polypyrazolylborato ligands of the type HB(pz)$_3$ · Hg–CN or pzB(pz)$_3$ · Hg–CN (pz = pyrazolyl or substituted pyrazolyl) have been synthesised and characterised by IR, conductivity, ^{1}H, ^{13}C, and ^{199}Hg NMR spectroscopy. The crystal structure of the cyanomercury hydridotris(1*H*-3,5-dimethylpyrazol-1-yl)borate has been resolved (space group $P\bar{1}$ with $a = 7.863(3)$, $b = 11.157(5)$, $c = 13.117(5)$ Å; $\alpha = 89.32(3)$, $\beta = 78.31(3)$, $\gamma = 79.13(4)°$, $V = 1106.22$ Å^3, $Z = 2$) showing a distorted tetrahedral coordination around Hg. The tris(pyrazolyl)borato complexes contain four-coordinated Hg and are rigid in solution at r.t., while the tetrakis(pyrazolyl)borates are fluxional. The ^{15}N-CPMAS-NMR spectrum of the pzTp · HgCN derivative suggests a tetracoordination around mercury in this complex in the solid state. © 1997 Elsevier Science S.A.

Keywords: Mercury; Boron; Poly(pyrazolyl)borates; X-ray; Solid state ^{15}N NMR

1. Introduction

Within the various d^{10} species the Hg(II) one occupies a special position in that high coordination numbers are seldom reached [1], except in a few cases when very poorly coordinating ligands are coupled with the bare Hg^{2+} ion [2]. The practical limit of tetracoordination is achieved mainly with good (soft) coordinating ligands (e.g. HgI_4^{2-}, $Hg(CN)_4^{2-}$, etc.) while tri- (often T-shaped) and (more often) dicoordination are quite common, not counting additional 'weak interactions' [3]. Trispyrazolylborato derivatives [1] are generally little investigated because of the oxidising properties of the mercury cationic moiety. It makes it difficult to obtain, especially in solution, stable complexes due to a facile reduction to metallic Hg at the expense of the *B*-bonded hydride oxidation according to the equation [2]

$$2HB(pz)_3^- + Hg^{2+} \rightarrow H_2 + 2B(pz)_3 + Hg$$

The ease of the reaction is also strongly dependent on the pyrazole (pz) substitution pattern. Such problems are obviously not present for tetrakis(pyrazolyl)borato ligands. The study of MeHg · pzTp [5,6] has revealed that Hg is T-shaped in the solid state and fluxional in solution down to −90 °C. A study on average coordination numbers in solution for organomercury complexes has been undertaken and useful correlations from NMR data have been found [7].

Previous investigations from these laboratories on polypyrazolylborato complexes of (organo)mercury(II)

* Corresponding author.

[1] The notation of Trofimenko [4] has been followed for each ligand while the generic tris(pyrazolyl)borate is denoted Tp$^{\#}$ and the tetrakis(pyrazolyl)borate pzTp$^{\#}$.

[2] The B(pz)$_3$ in water solution is rapidly hydrolysed to pyrazole and boric acid, while in inert organic solvents it generally dimerises to the pyrazabole [B(pz)$_3$]$_2$.

PII S0022-328X(97)00040-5

moieties [8–11] showed that the metal ion displays various coordination numbers and different fluxional behaviours. The same studies showed as well that these features depend on the nature of both the mercury cation and the ligand, so it was of interest to try and separate the ligand influence on coordination numbers and fluxionality in both solid state and solution from the mercury moiety contribution.

In order to better elucidate the ligand role, the cation NC–Hg^+ has been chosen since it is somewhat intermediate between 'inorganic' Hg^{2+} [8] and the R(Ar)–Hg^+ [9,11] which show quite different character in coordination ability and fluxional behaviour.

2. Experimental

Pyrazole, 3-methylpyrazole, 4-methylpyrazole and 3,5-dimethylpyrazole were commercially available (Aldrich) and were used as received. Carbon, hydrogen, and nitrogen analyses were carried out on a Fisons Instruments EA 1108 CHNS-O, infrared spectra were recorded from 4000 to 250 cm^{-1} on a Perkin–Elmer 2000 System Series FTIR instrument. The conductances of solutions (acetone) were measured with a Crison CDTM 522 conductimeter at room temperature.

2.1. NMR measurements

^1H, ^{13}C and ^{199}Hg solution NMR spectra were recorded at room temperature on a Varian VX-300 spectrometer operating at 299.95 MHz, 75.43 MHz, and 53.36 MHz respectively. The solid state NMR experiments were performed on a Jeol GSE 270 (6.34 T) spectrometer. Cylindrical 6 mm o.d. zirconia rotors with a sample volume of 120 μl were employed with a spinning speed in the range from 4.0 to 5.5 kHz. The magic angle was carefully adjusted from the ^{79}Br MAS (magic angle spinning) spectrum of KBr by maximising the number of rotational echoes visible in the resonance FID. High resolution solid state ^{15}N NMR were recorded at 27.4 MHz using the cross polarisation–magic angle spinning (CPMAS) technique. At least 12 h of accumulation were required to obtain a reasonable signal-to-noise ratio for ^{15}N spectra. Conditions for ^{15}N measurements were refined by using a 90% isotopically enriched $^{15}NH_4NO_3$ sample. ^{15}N chemical shifts are quoted relative to the signal of neat nitromethane ($\delta = 0$) using the high frequency positive convention.

2.2. Syntheses

The preparation of potassium salts of the tris(pyrazolyl)borato ligands has been accomplished according to established procedures [12,13], 3,4,5-trimethylpyrazole, 4-chloro-3,5-dimethylpyrazole together with the corresponding tris(pyrazolyl)borato ligands were prepared as described in previous papers [14]. KpzTp was prepared according to Ref. [12], while $KpzTp^{4Me}$ has been prepared as previously reported [15]. Solvent evaporations were always carried out in vacuo (water aspirator).

2.2.1. *Cyano[hydridotris(1H-pyrazol-1-yl)borato]mercury(II)* **1**

A solution of 0.252 g (1 mmol) of KTp in 20 ml of water was added to 20 ml of an aqueous solution of $Hg(CN)_2$ (0.253 g, 1 mmol) under stirring. A white precipitate soon formed which was recovered by filtration and quickly dried after washing with water and a methanol–water solution (ca. 4:1 v/v). At variance with the other compounds similarly prepared (**2**, **3**), the crude product was reprecipitated by adding petroleum ether to a solution in dichloromethane. Compound **2** was recrystallised from dichloromethane–acetonitrile, while crystals of **3**, suitable for X-ray analysis, were obtained from dichloromethane–cyclohexane.

2.2.2. *Cyano[hydridotris(3,4,5-trimethyl-1H-pyrazol-1-yl)borato]mercury(II)* **4**

$Hg(CN)_2$ (0.253 g, 1 mmol) and KTp^{*Me} (0.378 g, 1 mmol) were added to 30 ml of dichloromethane. The resulting solution/suspension was left for ca. 20 min under stirring; the formed KCN precipitate was filtered off and the filtrate was evaporated to dryness. The residue was purified by recrystallisation from dichloromethane/*n*-hexane. Compounds **5**, **6**, and **7** were obtained similarly. Compounds **2** and **3** were also synthesised in this manner.

2.3. X-ray crystallographic analysis

Crystal and experimental data are summarised later in Table 4. A crystal of $(BN_7C_{16}H_{21}Hg) \cdot 1/2(C_6H_{12})$ (compound **3**) obtained from a solution of CH_2Cl_2/cyclohexane was mounted on a Syntex $P2_1$ automatic four-circle diffractometer using graphite monochromated Mo radiation ($\lambda K\alpha = 0.71069$ Å). The cell parameters were refined by least-squares from the angular positions of 25 reflections in the range $16° < 2\theta < 32°$. The data were measured at room temperature for $5° < 2\theta < 120°$ from a crystal of approximate dimensions $0.25 \times 0.2 \times 0.05$ mm^3 using the $\theta/2\theta$ scan technique. The scan rate was automatically chosen according to the peak intensity in the range 3.0–15.0° min^{-1} and background counts were taken with a stationary crystal at each end of the scan and a total background time to scan time ratio of 0.5.

The data were processed to yield values of I and $\sigma(I)$. The intensities of three standard reflections, measured every 97 reflections throughout the data collection, decayed by about 30.0%. The values of I and

$\sigma(I)$ were corrected for Lorentz, polarisation decay and shape anisotropy [16] effects. A total of 2141 independent reflections having $I > 3\sigma(I)$ were used in all subsequent calculations. The mercury atom and 88% of the non-H atoms of the compound were located by the atomic PLUTO procedure [17] and successive structure factor calculations and Fourier maps provided the complete structure including a molecule of solvent. All non-hydrogen atoms were refined by full-matrix least-squares methods with anisotropic thermal parameters. The hydrogen atoms were idealised (C–H = 0.96 Å) and each H atom was assigned the equivalent isotropic temperature factor of the parent atom and allowed to ride on it. The final difference Fourier map, with a root-mean-square deviation of electron density of 0.23 e $Å^{-3}$, showed no significant features. Atomic scattering factors were taken from Ref. [18]. Calculations were performed on the DEC 3500 AXP, using the SIR CAOS [19] structure determination package.

3. Results and discussion

In order to avoid metallic mercury deposition it is necessary to choose the quickest possible synthesis for the complexes of the general type X–Hg · $Tp^{\#}$ [X = Hal, pseudo-Hal, NO_3, R, Ar, R–S, Ar–S; $Tp^{\#}$ here refers only to those featuring a hydridic *B*–H]. Two main synthetic pathways have so far been exploited.

$$\left[(X\text{–}Hg)^{+}_{aq}Y^{-}_{aq}\right] + K^{+}_{aq}(Tp^{\#})^{-}_{aq} \xrightarrow{H_2O} K^{+}_{aq}Y^{-}_{aq} + X\text{–}Hg \cdot Tp^{*}\downarrow \quad (1')$$

$$\left[(X\text{–}Hg\text{–}X_{aq}\right] + K^{+}_{aq}(Tp^{\#})^{-}_{aq} \xrightarrow{H_2O} K^{+}_{aq}X^{-}_{aq} + X\text{–}Hg \cdot Tp^{\#}\downarrow \quad (1'')$$

$$X\text{–}Hg\text{–}Y + KTp^{\#} \xrightarrow{CH_2Cl_2} KY\downarrow + X\text{–}Hg \cdot Tp^{\#} \quad (2)$$

Route (1) consists of the reaction in aqueous medium of a water soluble Hg precursor with a water soluble $KTp^{\#}$. The formation of the complex (independently of whether the Hg species in water is ionised or not) is usually immediate and its rapid precipitation preserves it from decomposition (decomposition in the solid state is much slower). In the second route (2) the reaction in dichloromethane solution/suspension of a partially soluble mercury precursor with a partially soluble $KTp^{\#}$ affords the soluble complex, while KY precipitates out. The reaction usually proceeds smoothly and may be faster than that in route (1) depending on ligand solubilities in the different media.

The first method was found to be suitable and ap-

Table 1
Yields, analyses, and physical properties and IR of compounds

	Compound [a]	Yield	M.p. (°C)	Elemental analysis (Found/Calc.) (%)			Λ [c]	IR			
				C	H	N		ν(C–H) pyrazole	B–H	1500–1600	Others ν(C≡N)
1	N≡C–Hg · Tp	88	[b]	27.5 27.3	2.3 2.3	22.1 22.3	1.30 (1.00)	3117 w	2492 m	1501 s	2174 m
2	N≡C–Hg · Tp^{Me}	86	[b]	32.6 32.4	3.5 3.4	20.4 20.5	1.40 (0.99)	3135s w	2463 m	1510 s	2176 w
3	N≡C–Hg · Tp^{*}	90	[b]	36.4 36.7	4.3 4.2	18.5 18.7	4.10 (1.02)	3122 w	2506 m	1515 m	2176 m
4	N≡C–Hg · Tp^{*Me}	70	[b]	40.5 40.3	5.2 5.0	17.1 17.3	1.60 (0.98)	—	2461 m	1580 m	2178 m
5	N≡C–Hg · Tp^{*Cl}	74	[b]	30.9 30.6	3.1 3.1	15.4 15.6	4.00 (1.04)	—	2484 s	1530 m	2180 m
6	N≡C–Hg · pzTp	72	197–199	31.0 30.9	2.5 2.4	25.1 24.9	1.40 (1.10)	3125 w	—	1510 s	2174 w
7	N≡C–Hg · $pzTp^{4\text{-}Me}$	68	188–190	35.9 36.1	3.7 3.6	24.5 24.8	3.20 (1.00)	3110 w	—	1508 s	2180 w

[a] Tp is hydridotris(-1*H*-pyrazol-1-yl)borate, $C_9H_{10}N_6B$; Tp^{Me} is hydrotris(3-methylpyrazol-1-yl)borato, $C_{12}H_{16}N_6B$; Tp^{*} is hydrotris(3,5-dimethylpyrazol-1-yl)borato, $C_{15}H_{22}N_6B$; Tp^{*Me} is hydrotris(3,4,5-trimethylpyrazol-1-yl)borato, $C_{18}H_{28}N_6B$; Tp^{*Cl} is hydrotris(3,5-dimethyl-4-chloropyrazol-1-yl)borato, $C_{15}H_{19}Cl_3N_6B$; pzTp is tetrakis(pyrazol-1-yl)borato, $C_{12}H_{12}N_8B$; $pzTp^{4Me}$ is tetrakis(4-methylpyrazol-1-yl)borato, $C_{16}H_{20}N_8B$.

[b] These compounds char without melting.

[c] Specific conductivity in acetone solution (Ω^{-1} cm^2 mol^{-1}) at room temperature and the molar concentration × 10^{-3} indicated in parentheses in the lower line.

Table 2
^{1}H and ^{199}Hg NMR data [a,b]

No.	Compound	H-3 or -5		H-4	3- or 5-Me		4-Me	^{199}H
		δ	δ	δ				δ [c]
1	N≡C–Hg · Tp	7.77 (7.5)	7.62 (8.1)	6.30 (13.4)	—	—	—	−1049.8
2	N≡C–Hg · Tp^{3Me}	—	7.58 (6.8)	6.04 (15.7)	2.36	—	—	−998.9
3	N≡C–Hg · Tp^{*}	—	—	5.81 (16.6)	2.29 (4.2)	2.37	—	−974.1
4	N≡C–Hg · Tp^{*Me}	—	—	—	2.28 (4.2)	2.22	1.84	−966.2
5	N≡C–Hg · Tp^{*Me}	—	—	—	2.30 (3.1)	2.75	—	−1011.1
6	N≡C–Hg · pzTp	7.75 [d]	7.73	6.39	—	—	—	−1074.3
		7.70 br [e]	7.50 br	6.39	—	—	—	
		7.65 br [f]	7.39 br	6.42 br	—	—	—	
		7.64 v br [g]	7.38 v br	6.43 v br	—	—	—	
7	N≡C–Hg · $pzTp^{4Me}$	7.50 [d]	7.31	—	—	—	2.07	−1066.1
		7.49 [e]	7.15 br	—	—	—	2.04	
		7.46 br [f]	7.03 br	—	—	—	2.03 br	
		7.40 br [g]	6.92 v br	—	—	—	2.02 br	

[a] $CDCl_3$ has been used as a solvent for all compounds. With temperatures below −40 °C CF_2/Br_2 has been added up to 3:1 v/v.
[b] $|^{2(or\ 3)}J|(^{199}Hg–^{1}H)$ in Hz are given in parentheses next to the corresponding δ values, where observed.
[c] Chemical shift values referenced to external neat $HgMe_2$ (δ = 0 ppm).
[d] r.t.; [e] −30 °C; [f] −50 °C; [g] −80 °C.

plied for compounds **2–3** and the second one for compounds **2–7** of Table 1. Compound **1**, prepared according to the first method, requires special care in order to avoid the aforementioned decomposition [8,10,11]. Interestingly, no other 'inorganic' derivative of formula X–Hg · Tp (X ≠ CN) has been obtained following similar procedures.

IR spectra show the expected bands for the *pz*-C–H, B–H, and C≡N stretchings and the pyrazole 'ring breathing' vibrations at 1500–1600 cm^{-1}, as reported in Table 1.

3.1. Solution NMR

^{1}H, ^{13}C and ^{199}Hg NMR data are shown in Tables 2 and 3. The number of resonances and their chemical shifts indicate that in the case of hydridotris(pyrazolyl)borato complexes as well as in the case of tetrakis(pyrazolyl)borato ones in the solution state all the pyrazolyl moieties are equivalent within the NMR timescale. However, all the $Tp^{\#}$ complexes show couplings between the ^{199}Hg nucleus with the H-4 of the pyrazole rings and some of them (**1–3**) with C-4 (see Tables 2 and 3). The size of the $|^{4}J|(^{199}Hg–^{1}H)$ and $|^{3}J|(^{199}Hg–^{13}C)$ reported here (13.4–16.6 Hz and 26.1–29.8 Hz respectively) are similar to the ones previously observed for corresponding non-fluxional complexes of the type X–Hg · $Tp^{\#}$ (11.0–24.0 Hz and 25.0–33.0 Hz respectively) [8]. The presence and the similarity of such couplings imply a rigidity of the coordination scheme in solution. Moreover, additional couplings of ^{199}Hg with the H-3 and/or H-5 are seen here for **1** (7.5 and 8.1 Hz) and **2** (6.8 Hz) which could not be observed in other X–Hg · $Tp^{\#}$ complexes [8]. On the other hand, the $pzTp^{\#}$ complexes did not show any detectable coupling constant between ^{199}Hg and the carbons or

Table 3
^{13}C NMR data [a,b]

No.	Compound	C-3	C-5	C-4	Me-3 or -5		Me-4	C≡N
		δ						
1	N≡C–Hg · Tp	141.2 (46.1)	136.2	105.0 (29.8)	—	—	—	132.2
2	N≡C–Hg · Tp^{3Me}	150.0	136.9	104.5 (26.7)	13.6	—	—	132.2
3	N≡C–Hg · Tp^{*}	148.8 (40.7)	145.6 (16.4)	105.1 (26.1)	12.8	13.5	—	133.1
4	N≡C–Hg · Tp^{*Me}	147.3	142.6	111.2	11.0	12.2	7.9	133.6
5	N≡C–Hg · Tp^{*Cl}	146.4	142.4	109.2	10.8	11.8	—	131.5
6	N≡C–Hg · pzTp	142.2	136.1	106.0	—	—	—	130.6
7	N≡C–Hg · $pzTp^{4Me}$	142.2	134.7	115.9	—	—	8.8	132.1
		141.9 [c]	134.9	114.9	—	—	8.9	128.2

[a] $CDCl_3$ has been used as a solvent for all compounds except where otherwise stated.
[b] $|^{2(or\ 3)}J|(^{199}Hg–^{13}C)$ in Hz are given in parentheses next to the corresponding δ values, where observed.
[c] r.t., in acetone.

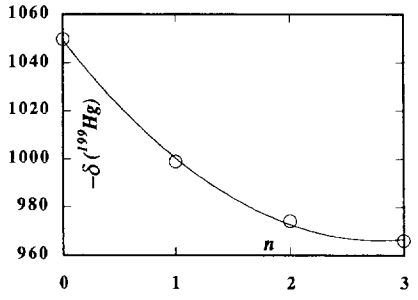

Fig. 1. Plot of the ^{199}Hg resonances in the compounds vs. the number n of Me groups as substituents in the pyrazolyl rings.

protons of the pyrazole rings. This feature, together with the apparent equivalence of the four pyrazole rings, is a clear indication of ligand exchange processes occurring at the metal centre. Such a behaviour has been probed by low temperature proton spectra down to −80 °C for the pzTp# complexes. The spectra show a progressive peak broadening till complete loss of their fine structure, and peak shifting, but no new peak is observed (for comparison, some low temperature spectra, up to −50 °C, of the non-fluxional NC–Hg · Tp* do not show any significant change from the one at room temperature). A similar trend is typical of organomercury poly(pyrazolyl)borates which have been shown to be fluxional down to −90 °C [6,9].

Heavy metal chemistry presents many problems of structure and bonding characterisation. For this reason, the direct ^{199}Hg study is particularly attractive, since spectra are usually sensitive to small electronic or stereochemical changes in the metal environment.

As can be seen in Table 2, the recorded values of the ^{199}Hg chemical shifts lie in a range which is characteristic of X–Hg–Tp# or X–Hg–pzTp# complexes [8,10,20]. Nevertheless, analysing such values as a function of the ligand substitution pattern shows than an approximate correspondence is found with the expected electronic variations at the Hg nucleus. Reporting the ^{199}Hg resonance in a plot (Fig. 1) against the number n of Me substituents in the pyrazole ring, a progressive increase of δ is observed with increasing n, i.e. with the potential donating ability of the relevant ligand. Moreover, the above ordering holds true also when in the same complexes the group Et–S– [10] is exchanged for the N≡C– one. Again, the value for NC–Hg · pzTp is higher than that for NC–Hg · pzTp^{4Me}. Thus, it appears that the ^{199}Hg resonance in a homogeneous series can be taken as an approximate indicator of the donating power of the ligand, and extrapolating the above findings, one would expect the value for NC–Hg · Tp*^{Cl} (**5**) to be higher than that of NC–Hg · Tp* (**3**). Its actual value indeed falls between those of Tp and Tp^{Me}, see Table 2. Similarly, the value for NC–Hg · pzTp (**6**) is found to be lower than the NC–Hg · Tp (**1**) one (the lower donating power of the pzTp relative to Tp has however been established independently [21]).

3.2. ^{15}N Solid state NMR

High resolution solid state NMR spectroscopy may be a powerful tool for the investigation of the chemical nature of the Hg–ligand interaction mainly because the fast exchange processes that prevent the interpretation of the coordination mode of the Hg atom in solution are usually frozen in the solid state. The technique can also be applied for poorly crystalline compounds that cannot be analysed by single crystal X-ray analysis. Of course the structure information found in the solid state may be different from the solution case since the solid lattice environment is expected to impose a tighter coordination scheme to the metallic centre.

^{15}N NMR measurements in natural isotopic conditions, that are often prevented in solution by the limited solubility of the compounds, may be obtained in the solid state in order to evaluate the coordination shift experienced by the *N*-donor atoms interacting with the metal atom.

In the absence of suitable crystals of NC–Hg · pzTp, analysis of its solid state ^{15}N NMR may afford valuable information on the Hg environment and coordination scheme.

Comparison of the ^{15}N CPMAS spectrum of the free and coordinated ligand can be a diagnostic tool for the elucidation of the ligand coordination around the metallic centre. As previously reported the ^{15}N CPMAS spectrum of the free pzTp ligand shows two peaks at −79 and −85 ppm, assigned to the {N(2)} atoms and a broader resonance at −154 ppm assigned to {N(1)} nuclei [20]. The spectrum of NC–Hg · pzTp shows four resonances at −72.1, −89.3, −106.4, and −159.4 ppm respectively, in an approximate relative ratio 1:1:3:4 (Fig. 2). The resonances of {N(1)} nuclei in the pzTp

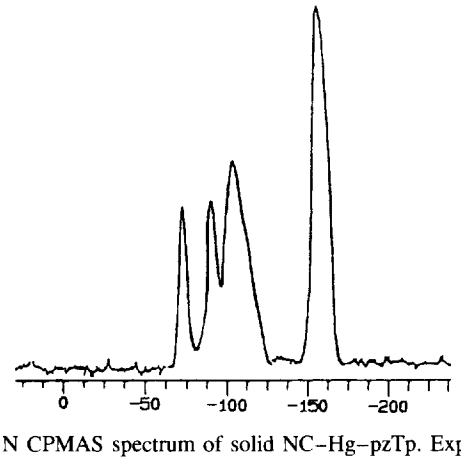

Fig. 2. ^{15}N CPMAS spectrum of solid NC–Hg–pzTp. Experimental conditions: spinning speed 4.87 kHz, recycle time 15 s, contact time 5 ms.

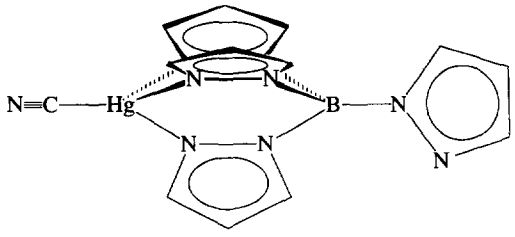

Fig. 3. Schematic mercury coordination environment in pzTp·Hg–CN.

ligand showed to be weakly affected by the coordination with a mercury atom [20]. On this basis we can assign the broad peak at −159.4 ppm to the four overlapping resonances of the N(1) atoms.

The signal located at −72.1 ppm shows a marked decrease of its intensity at short contact times (1–3 ms). On this basis, we can assign this resonance to the nitrogen atom of the cyano group since it lies far from intramolecular protons and then is expected to require longer contact times to allow magnetisation to be transferred. This resonance falls within the ^{15}N chemical shift range (−59 to −180 ppm) reported for cyano groups coordinated to metal atom [22]. As has previously been reported, the interaction of the nitrogen atoms of the polypyrazolylborato ligand with the metal centre causes a higher field shift of the ^{15}N resonances. Then the presence of the peak at −106.4 ppm and its relative intensity suggest the coordination of three almost equivalent nitrogen atoms to the metal to define, together with the C≡N group, a distorted tetrahedral environment around the Hg ion (Fig. 3).

In principle one should expect for the proposed structure two signals in the relative ratio 3:1 for the N(1) atoms, but the broad signal at −149.4 ppm does not allow us to distinguish the two different environments.

Furthermore the broadness of the peak at −106.4 ppm in the ^{15}N CPMAS spectrum of the NC–Hg · pzTp derivative may be due to crystallographic disorder or small inequivalences in the Hg–N bond lengths.

All attempts to observe solid state ^{199}Hg NMR spectra of the complex were unsuccessful probably because of the large chemical shift anisotropy of the metal centre.

3.3. Description of the molecular structure

A perspective drawing of the compound is shown in Fig. 4(a)–(b) together with the numbering scheme adopted. Crystallographic data are reported in Table 4, final atomic coordinates and equivalent isotropic thermal parameters with standard deviations are listed in Table 5, while some relevant interatomic distances and angles are reported in Table 6. The crystal structure consists of molecules of $HB(3,5\text{-}Me_2Pz)_3 \cdot HgCN$ and molecules of cyclohexane in 2:1 ratio. The coordination geometry at the Hg atom can be considered as a distorted tetrahedron with one Hg–N bond longer

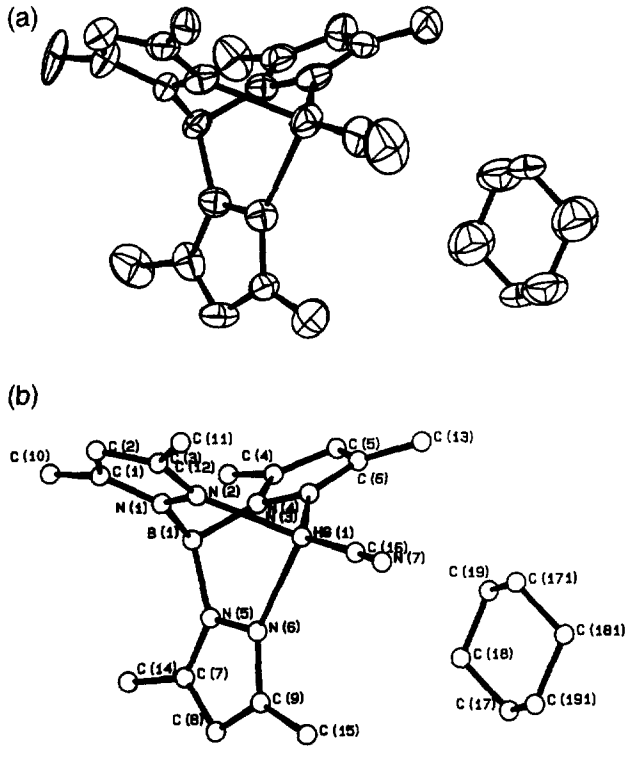

Fig. 4. (a) Molecular structure of the compound and (b) labelling scheme drawn with 50% thermal ellipsoids.

Table 4
Crystallographic data

mol formula	$(HgBN_7C_{16}H_{21})\cdot 1/2(C_6H_{12})$
mw	565.250
crystal system	triclinic
space group	$P\bar{1}$
a (Å)	7.863(3)
b (Å)	11.157(5)
c (Å)	13.117(5)
α, β, γ (deg)	89.32(3), 78.31(3), 79.13(4)
V (Å^3)	1106.22
Z	2
ρ(calc) (g cm^{-3})	1.696
μ (cm^{-1})	71.225
F(000)	550.00
no. of measured reflections	3553
no. of unique reflections	3136
observed reflections [$I > 3\sigma(I)$]	2141
function minimized	$\Sigma w(\|F_o\| - \|F_c\|)^2$
variables refined	250
a, b, c values in the weight function $w = 1.0/(a + bF_o + cF_o)$	0.00000, 0.17932, 0.00246
final R [a]	0.057
final Rw [a]	0.076
goodness of fit s [b]	1.0

[a] $R = \Sigma|F_o - F_c|/\Sigma F_o$; $Rw = \{\Sigma w(|F_o| - |F_c|)^2/\Sigma w|F_o|^2\}^{1/2}$.
[b] $s = \{\Sigma w(|F_o| - |F_c|)^2/(N_{refl} - N_{param})\}^{1/2}$.

Table 5
Atomic coordinates and isotropic thermal parameters B_{eq} (Å^2) of the non-hydrogen atoms (e.s.d.s in parentheses) [a]

Atom	x	y	z	B_{eq}
HG(1)	0.3882(1)	0.3178(1)	0.5760(1)	3.32(2)
B(1)	0.351(3)	0.156(2)	0.789(1)	2.9(5)
N(1)	0.537(2)	0.177(1)	0.762(1)	2.7(4)
N(2)	0.592(2)	0.242(1)	0.671(1)	2.9(4)
N(3)	0.217(2)	0.277(1)	0.808(1)	2.6(4)
N(4)	0.213(2)	0.362(1)	0.729(1)	3.0(4)
N(5)	0.305(2)	0.080(1)	0.703(1)	2.8(4)
N(6)	0.304(2)	0.128(1)	0.606(1)	2.8(4)
N(7)	0.476(4)	0.409(2)	0.349(2)	7.4(9)
C(1)	0.686(2)	0.139(2)	0.802(1)	3.6(5)
C(2)	0.821(3)	0.182(2)	0.747(2)	4.2(6)
C(3)	0.763(2)	0.247(1)	0.664(1)	3.5(5)
C(4)	0.093(2)	0.323(1)	0.895(1)	3.5(5)
C(5)	0.008(3)	0.435(2)	0.870(1)	3.8(5)
C(6)	0.082(2)	0.457(1)	0.769(1)	3.3(5)
C(7)	0.272(2)	−0.033(1)	0.705(1)	3.3(5)
C(8)	0.248(3)	−0.059(2)	0.606(2)	4.0(6)
C(9)	0.265(2)	0.042(1)	0.549(1)	3.1(5)
C(10)	0.670(3)	0.071(2)	0.903(2)	6.0(7)
C(11)	0.864(2)	0.314(1)	0.579(1)	3.5(7)
C(12)	0.067(3)	0.255(2)	0.992(1)	5.0(7)
C(13)	0.036(3)	0.566(2)	0.707(2)	4.8(6)
C(14)	0.273(3)	−0.119(2)	0.798(2)	5.3(7)
C(15)	0.257(3)	0.066(2)	0.436(2)	4.9(6)
C(16)	0.439(3)	0.380(2)	0.430(1)	4.6(7)
C(17)	0.411(2)	0.405(1)	−0.004(1)	3.3(5)
C(18)	0.510(2)	0.413(1)	0.072(1)	6.6(9)
C(19)	0.511(3)	0.539(2)	0.096(2)	5.9(8)

[a] $B_{eq} = 4/3\Sigma_i\Sigma_j \beta_{ij} a_i a_j$.

(2.34(1) Å) than the other two (2.26(1), 2.20(2) Å). The N–Hg–N angles are not significantly different (82.0(5), 83.5(5), 83.7(5)°) while the three N–Hg–C angles have different values (120.6(6), 125.9(9), 142.1(8)°), the smallest of them corresponding to the longest Hg–N distance. The geometry is similar to the closely related complex of a tripodal ligand $[MeHg(py)_3COH]^+NO_3^-$ which has Hg–N = 2.28(1)–2.53(1) Å, C–Hg–N = 119(1)–150(1)° [23]. The coordination of the B-atom is quite normal and the three pyrazole rings are planar within the limits of experimental error. The distances of the Hg atom from the mean plane of the pyrazole rings are: −0.0322 [ring containing N(2)], −0.0716 [ring containing N(4)], and 0.2365 (ring containing N(6)], reflecting weaker mercury–nitrogen bonding with the latter donor atom. The geometry of the cyclohexane (from the crystallisation mixture) does not present irregularities. Such a distorted tetrahedral structure displays Hg–N bond distances and C–Hg–N angles which are much more regular than those in MeHgpzTp [6], which contain an essentially dicoordinated Hg, but also in $[MeHg(2,2'\text{-bpy})]^+$ [24] and/or $[MeHg(py)_2CH_2]^+$, and $[MeHg(Et_3terpy)]^+$ [25], $[MeHg(py)_3COH]^+$ and $[MeHg(py)_2(N\text{-MeIm})COH]^+$ [23]. The latter two structures have been inserted in Table 7 together with the present one in order to compare some characteristic features. As can be seen, the $[MeHg(py)_2(N\text{-MeIm})COH]^+$ structure contains a very close Hg–N(A) distance coupled with a C–Hg–N(A) angle of 170°, while the distances Hg–N(B) and Hg–N(C) (2.66–2.71 Å) are much greater and each other similar. Furthermore, the displacements of the Hg atom from the mean planes containing the three rings follow a trend similar to the relevant Hg–N distances: they increase by ca. an order of magnitude in passing from the ring with N(A) to the other two. This allows us to describe the

Table 6
Selected bond distances (Å) and bond angles (°) with e.s.d.s in parentheses

Bond distance			
HG(1)–N(2)	2.26(1)	C(3)–N(2)	1.34(2)
HG(1)–N(4)	2.20(2)	N(1)–N(2)	1.42(2)
HG(1)–N(6)	2.34(1)	C(4)–C(5)	1.37(3)
HG(1)–C(16)	2.01(2)	C(4)–C(12)	1.47(3)
N(1)–N(2)	1.42(2)	C(4)–N(3)	1.37(3)
N(1)–B(1)	1.50(3)	C(5)–C(6)	1.37(3)
N(3)–N(4)	1.39(2)	C(6)–C(13)	1.48(3)
N(3)–B(1)	1.54(3)	C(6)–N(4)	1.36(3)
N(5)–N(6)	1.38(2)	N(3)–N(4)	1.39(2)
N(5)–B(1)	1.55(2)	C(7)–C(8)	1.39(3)
N(7)–C(16)	1.11(3)	C(7)–C(14)	1.54(3)
C(1)–C(2)	1.32(3)	C(7)–N(5)	1.34(2)
C(1)–C(10)	1.52(3)	C(8)–C(9)	1.36(2)
C(1)–N(1)	1.38(2)	C(9)–C(15)	1.51(3)
C(2)–C(3)	1.42(3)	C(9)–N(6)	1.34(2)
C(3)–C(11)	1.51(3)	N(5)–N(6)	1.38(2)
C(17)–C(18)	1.40(2)		
C(18)–C(19)	1.44(3)		
C(19)–C(17′)	1.43(3)		
Bond angles			
N(4)–HG(1)–N(2)	83.7(5)	N(2)–C(3)–C(2)	107(1)
N(6)–HG(1)–N(2)	83.5(5)	N(2)–C(3)–C(11)	122(1)
N(6)–HG(1)–N(4)	82.0(5)	N(2)–N(1)–C(1)	105(1)
C(16)–HG(1)–N(2)	125.9(9)	N(1)–N(2)–C(3)	108(1)
C(16)–HG(1)–N(4)	142.1(8)	N(3)–C(4)–C(5)	107(1)
C(16)–HG(1)–N(6)	120.6(6)	N(3)–C(4)–C(12)	122(1)
N(3)–B(1)–N(1)	111(1)	C(12)–C(4)–C(5)	130(2)
N(5)–B(1)–N(1)	111(1)	C(6)–C(5)–C(4)	107(1)
N(5)–B(1)–N(3)	108(1)	C(13)–C(6)–C(5)	128(1)
N(1)–N(2)–HG(1)	118(1)	N(4)–C(6)–C(5)	109(1)
N(3)–N(4)–HG(1)	119(1)	N(4)–C(6)–C(13)	121(1)
N(5)–N(6)–HG(1)	117.6(8)	N(4)–N(3)–C(4)	109(1)
N(7)–C(16)–HG(1)	176(2)	N(3)–N(4)–C(6)	105(1)
N(2)–N(1)–B(1)	119(1)	N(5)–C(7)–C(8)	106(1)
N(4)–N(3)–B(1)	120(1)	N(5)–C(7)–C(14)	125(1)
N(6)–N(5)–B(1)	119(1)	C(14)–C(7)–C(8)	128(1)
C(16)–HG(1)–B(1)	167.0(7)	C(9)–C(8)–C(7)	107(1)
N(1)–C(1)–C(2)	110(1)	C(15)–C(9)–C(8)	130(1)
N(1)–C(1)–C(10)	118(1)	N(6)–C(9)–C(8)	110(1)
C(10)–C(1)–C(2)	130(1)	N(6)–C(9)–C(15)	118(1)
C(3)–C(2)–C(1)	107(1)	N(6)–N(5)–C(7)	110(1)
C(11)–C(3)–C(2)	129(1)	N(5)–N(6)–C(9)	105(1)
C(19)–C(18)–C(17)	110(1)		
C(17′)–C(19)–C(18)	109(1)		
C(18′)–C(17′)–C(19)	108(1)		

Table 7
Comparison of selected structural data for complexes with tridentate nitrogen donor ligands

[a]	NC–Hg · Tp*	[Me–Hg · $(py)_3$COH]NO_3	[Me–Hg · $(py)_2$(*N*-MeIm)COH]NO_3
Hg–C (Å)	2.01(2)	2.03(2)	2.05(1)
Hg–N(A) (Å)	2.20(2)	2.28(1)	2.13(1)
C–Hg–N(A) (deg)	142.1(8)	150(1)	170(0)
Hg · · · plane (Å)	−0.0716(8)	−0.054(1)	0.075(0)
Hg–N(B) (Å)	2.26(1)	2.45(1)	2.66(1)
C–Hg–N(B) (deg)	125.9(9)	132(1)	110(0)
Hg · · · plane (Å)	−0.0322(6)	0.349(1)	−0.612(0)
Hg–N(C) (Å)	2.34(1)	2.53(1)	2.71(1)
C–Hg–N(c) (deg)	120.6(6)	119(1)	114(0)
Hg · · · plane (Å)	0.2365(9)	0.590(1)	−1.136(0)
Ref.	this work	[23]	[23]

[a] The N(A)–N(C) are given according to increasing Hg–N distance.

structure as one in which only one strong Hg–N bond is present (that with the imidazolic N, which notoriously is a much better donor than the pyridinic one). The C–Hg–N is almost linearly arranged, plus two other much weaker Hg · · · N interactions. The $[MeHg(py)_3COH]^+$ structure, although more regular (the C–Hg–N(A) angle is 150°), shows distances Hg–N(B) and Hg–N(C) (2.45–2.53 Å) which, compared with Hg–N(A), are however distinctly greater. Moreover, the displacements of the Hg atom from the mean planes still follow (though attenuated) an analogous ordering. In the present structure the C–Hg–N(A) angle is smaller and the Hg–N distances increase only approximately linearly from 2.20 to 2.34 Å. Here only the displacement of the Hg atom from the mean plane of the ring containing N(C) is ca. an order of magnitude greater than that of N(B) or N(A) (but its value is less than half that in the latter structure). This allows us to consider the present structure as one featuring at least two strong bonds between Hg and N with the third one less strong, but not a mere weak interaction.

3.4. Concluding remarks

The Tp or pzTp complexes investigated in this study appear to contain four-coordinate mercury atoms in the solid state. In solution their behaviour is different since the $pzTp^{\#}$ complexes are clearly fluxional while $Tp^{\#}$ complexes show a rigid coordination scheme at room temperature. By considering the coordination number in the solid state we conclude that an electron releasing group (Me [6,20], 5-Me–thienyl [11]) attached to Hg or a poorly electron withdrawing one (R–S– [20]) favour a substantial dicoordination or at most a T-shaped tricoordination, while stronger electron withdrawing ones (halogen [8], NC–) induce tetracoordination even with the ligand pzTp. This may be rationalised in terms of (i) high promotion energies of Hg 6s electrons, (ii) electronic demand of the Hg cationic moiety, and (iii) the donor power of the anionic ligand. When both the electronic demand of the Hg moiety and the donor power of the ligand are weak, the mercury atom prefers a coordination scheme involving two strong bonds plus other essentially electrostatic interactions. In this case, the formation of four weak bonds should not compensate the high promotion energetic costs. On the other hand, if the electronic demand of the metal centre and the ligand donor ability are strong enough, the formation of four full bonds is capable of compensating the promotion expenses. In the cases already examined the electronic demand may be (approximately) ordered as follows: $R–Hg^+ \leq Ar–Hg^+ \leq R(Ar)–S–Hg^+ < NC–Hg \leq Cl–Hg^+ < Me–CO–O–Hg^+ < O_2N–O–Hg^+ < O_3Cl–O–Hg^+$, while the donor ability is $pzTp < pzTp^{4Me} < Tp < Tp^{Me} < Tp^*$. In the present case the cyano group linked to mercury seems sufficiently strong an electron withdrawer to induce three pyrazole N atoms to fully bind to the metal at least in the solid state.

4. Supplementary material available

Tables of observed and calculated structure factors, anisotropic thermal parameters for non-H atoms as well as hydrogen atom parameters are available as supplementary material from the Editor.

Acknowledgements

The University of Camerino, University of Torino and Consiglio Nazionale deile Ricerche (CNR) are gratefully acknowledged.

References

[1] A.J. Canty, G.B. Deacon, Inorg. Chim. Acta 45 (1980) L225.
[2] R. Åkesson, M. Sandström, C. Stålhandske, I. Persson, Acta Chem. Scand. 45 (1991) 165.
[3] D.P. Graddon, Rev. Inorg. Chem. 4 (1982) 211.
[4] S. Trofimenko, Chem. Rev. 93 (1993) 943.
[5] A.J. Canty, N.J. Minchin, J.M. Patrick, A.H. White, Aust. J. Chem. 36 (1983) 1107.
[6] A.J. Canty, B.W. Skelton, A.H. White, Aust. J. Chem. 40 (1983) 1609.
[7] A.J. Canty, C.V. Lee, Organometallics 15 (1982) 1063; D.L. Rabenstein, Acc. Chem. Res. 11 (1978) 100; D.L. Rabenstein, J. Chem. Educ. 55 (1978) 292.
[8] G. Gioia Lobbia, F. Bonati, P. Cecchi, C. Pettinari, Gazz. Chim. Ital. 121 (1991) 355.
[9] G. Gioia Lobbia, P. Cecchi, F. Bonati, G. Rafaiani, Synth. React. Inorg. Met-Org. Chem. 22 (1992) 775.
[10] G. Gioia Lobbia, P. Cecchi, S. Bartolini, C. Pettinari, A. Cingolani, Gazz. Chim. Ital. 123 (1993) 641.
[11] G. Gioia Lobbia, P. Cecchi, F. Giordano, C. Santini, J. Organomet. Chem., 515 (1996) 213.
[12] S. Trofimenko, J. Am. Chem. Soc. 22 (1967) 6288.
[13] G. Gioia Lobbia, S. Calogero, B. Bovio, P. Cecchi, J. Organomet. Chem. 440 (1992) 27.
[14] G. Gioia Lobbia, P. Cecchi, R. Spagna, M. Colapietro, A. Pifferi, C. Pettinari, J. Organomet. Chem. 485 (1995) 45; D.U. O'Brien, C. Hrung, J. Organomet. Chem. 27 (1971) 185; S. Calogero, G. Gioia Lobbia, P. Cecchi, G. Valle, J. Friedl, Polyhedron 13 (1994) 87.
[15] G. Gioia Lobbia, P. Cecchi, C. Santini, S. Calogero, G. Valle, F.E. Wagner, J. Organomet. Chem., 513 (1996) 139.
[16] A.C.T. North, D.C. Phillips, F. Scott Mathews, Acta Crystallogr. A24 (1968) 351.
[17] M. Camalli, R. Spagna, J. Appl. Cryst. 27 (1994) 861.
[18] International Tables for X-ray Crystallography, vol. IV, Kynoch Press, Birmingham, 1974, p. 99.
[19] M. Camalli, D. Capitani, G. Cascarano, S. Cerrini, C. Giacovazzo, R. Spagna, Ital. Pat. No. 35403c/86; SIR CAOS User Guide, Istituto di Strutturistica Chimica CNR.
[20] S. Aime, G. Digilio, R. Gobetto, P. Cecchi, G. Gioia Lobbia, M. Camalli, Polyhedron 13 (1994) 2695.
[21] C. Lopez, R.M. Claramunt, D. Sanz, C. Foces Foces, F.H. Cano, R. Faure, E. Cayon, J. Elguero, Inorg. Chim. Acta 176 (1990) 195.
[22] J. Mason, in J. Mason (Ed.), Multinuclear NMR, Plenum Press, New York, 1987; A.J. Deeming, S. Donovan-Mtunzi, J. Chem. Soc., Dalton Trans. (1985) 1609.
[23] A.J. Canty, N. Chaichit, B.M. Gatehouse, E.E George, Inorg. Chem. 20 (1981) 4293.
[24] A.J. Canty, B.M. Gatehouse, J. Chem. Soc., Dalton Trans. (1976) 2018.
[25] A.J. Canty, N. Chaichit, B.M. Gatehouse, E.E George, Inorg. Chem. 20 (1981) 2414.